Graviton production by two photon and electron-photon processes in Kaluza-Klein theories with large extra dimensions

David Atwood*
Department of Physics and Astronomy, Iowa State University, Ames, Iowa 50011

Shaouly Bar-Shalom†
Department of Physics, University of California, Riverside, California 92521

Amarjit Soni‡
Theory Group, Brookhaven National Laboratory, Upton, New York 11973
(Received 21 September 1999; published 10 May 2000)

We consider the production of gravitons via two photon and electron-photon fusion in Kaluza-Klein theories which allow TeV scale gravitational interactions. We show that at electron-positron colliders, the processes $l^+l^- \to l^+l^- +$ graviton, with $l=e,\ \mu$, can lead to a new signal of low energy gravity of the form $l^+l^- \to l^+l^- +$ missing energy which is well above the standard model background. For example, with two extra dimensions, at the Next Linear Collider with a center of mass energy of 500 or 1000 GeV, hundreds to thousands such $l^+l^- +$ graviton events may be produced if the scale of the gravitational interactions, M_D, is around a few TeV. At a gamma-electron collider, more stringent bounds may be placed on M_D via the related reaction $e^-\gamma \to e^- G$. For instance, if a 1 TeV e^+e^- collider is converted to an electron-photon collider, a bound of $\sim 10(14)$ TeV may be placed on the scale M_D if the number of extra dimensions $\delta=2$, while a bound of $\sim 4(5)$ TeV may be placed if $\delta=4$, with unpolarized (right polarized) electron beams.

PACS number(s): 11.10.Kk, 04.50.+h, 11.25.Mj, 13.10.+q

I. INTRODUCTION

Gravity is the weakest force of nature and, although it ultimately controls the shape of the entire universe, its role in fundamental interactions remains obscure. This is due to the fact that gravity is expected to remain weak until the unreachably high scale of the Planck mass and thus there is no experimental data to construct a theory of gravity at small distances.

Of course the lack of experimental evidence has not deterred the construction of theories to account for the properties of gravitation at short distances. In this paper we will consider certain Kaluza-Klein theories which contain compact dimensions in addition to the $(3+1)$ space-time dimensions.

In such theories it was traditionally assumed that the compact dimensions form a manifold which is unobservably small (perhaps at the Planck scale) and thus remain hidden. However, recent advances in M theory [1], a Kaluza-Klein theory in which there are 11 total dimensions, suggest another possible scenario [2]. In models proposed in [2,3], δ of these extra dimensions may be relatively large while the remaining dimensions are small. In this class of theories, the known fermions, the strong, weak and electromagnetic forces exist on a 3-brane while gravity may act in $4+\delta$ dimensions. The size of these extra dimensions, R, is related to an effective Planck mass M_D according to [2]

$$8\pi R^{\delta} M_D^{2+\delta} \sim M_P^2 \tag{1}$$

where $M_P = 1/\sqrt{G_N}$ is the Planck mass and G_N is Newton's constant. Indeed the effective Planck mass at which gravitational effects become important may be as small as $O(1\ \text{TeV})$ in which case such effects may be probed in collider experiments.

In this scenario, at distances $d<R$ the Newtonian inverse square law will fail [2]. If $\delta=1$ and $M_D=1$ TeV, then R is of the order of 10^8 km, large on the scale of the solar system, which is clearly ruled out by astronomical observations. However, if $\delta \geqslant 2$ then $R<1$ mm; there are no experimental constraints on the behavior of gravitation at such scales [5] so these models are possible.

Astonishingly enough if $M_D \sim 1$ TeV then gravitons may be readily produced in accelerator experiments. This is because the extra dimensions give an increased phase space for graviton radiation. Another way of looking at this situation is to interpret gravitons which move parallel to the 4 dimensions of space time as the usual gravitons giving rise to Newtonian gravity while the gravitons with momentum components perpendicular to the brane are effectively a continuum of massive objects. The density of gravitons states is given by [2,3,6,7] where in particular we use the convention of [6]:[1]

*Email address: atwood@iastate.edu
†Email address: shaouly@phyun0.ucr.edu
‡Email address: soni@bnl.gov

[1]In [7] the scale of the extra dimension is parametrized by M_S which is related to M_D used here via $M_D^{\delta+2} = (S_{\delta-1}/16\pi) M_S^{\delta+2}$; in particular, if $\delta=2,4,6,8$ then $M_D \approx (0.59, 0.86, 0.94, 0.96) M_S$. The results quoted here in the M_D convention will thus become numerically somewhat larger when converted to the M_S convention. Note also that in [4] the scale of the extra dimension is parametrized by M which is related to M_D according to $M^{\delta+2} = 2M_D^{\delta+2}$.

$$D(m^2)=\frac{dN}{dm^2}=\frac{1}{2}S_{\delta-1}\frac{\bar{M}_P^2 m^{\delta-2}}{M_D^{\delta+2}} \tag{2}$$

where m is the mass of the graviton, $\bar{M}_P=M_P/\sqrt{8\pi}$ and $S_{\delta-1}=2\pi^{\delta/2}/\Gamma[\delta/2]$. The probability of graviton emission may thus become large when the sum over the huge number of graviton modes is considered.

Gravitons with polarizations that lie entirely within the physical dimensions are effective spin 2 objects which we consider in this paper. Gravitons with polarizations partially or completely perpendicular to the physical brane are vector and scalar objects which we will not consider here since they couple more weakly than the spin 2 type.

The compelling idea that gravity may interact strongly at TeV scale energies has recently led to a lot of phenomenological activity. TeV scale gravity can be manifested either directly through real graviton production, leading to a missing energy signal, or indirectly through virtual graviton exchanges. Thus, existing and future high energy colliders can place bounds (or detect) on the scale and the number of extra dimensions in these theories by looking for such signals [4,6–16].

Typically, direct signals drop as $(E/M_D)^{\delta+2}$, where E is the maximum energy carried by the emitted gravitons. Therefore, the best limits on M_D from the existing experimental data at the CERN e^+e^- collider LEP2, Fermilab Tevatron and DESY ep collider HERA are obtained for the case $\delta=2$. For example, existing LEP2 data on $\sigma(e^+e^-\to\gamma+\text{missing energy})$ already places the bound, $M_D\gtrsim 1$ TeV for $\delta=2$ via the process $e^+e^-\to\gamma+G$ (see Refs. [4,6,15]). For $\delta=4$ the limit is $M_D\gtrsim 700$ GeV. A Next Linear Collider (NLC) with c.m. energy $\gtrsim 1$ TeV can push this limit up to $M_D\gtrsim 6$ TeV (for $\delta=2$) and $M_D\gtrsim 4$ TeV (for $\delta=4$) [4]. In hadronic colliders, the signal $p\bar{p}\to\text{jet}+\text{missing energy}$ can proceed by the subprocesses $q\bar{q}\to gG$, $q(\bar{q})g\to q(\bar{q})G$ and $gg\to gG$. Using these, the existing Tevatron data on $\sigma(p\bar{p}\to\text{jet}+\text{missing energy})$ places the limits $M_D\gtrsim 750$ GeV for $\delta=2$ and $M_D\gtrsim 600$ GeV for $\delta=4$, while the LHC will be able to probe M_D up to ~ 7 TeV for $\delta=2$ [4,6].

The present bounds obtained from indirect signals associated with virtual graviton exchanges are typically $M_D\gtrsim 500-700$ GeV via processes such as $e^+e^-\to\gamma\gamma, ZZ, W^+W^-$ (LEP2) [14], $e^+q\to e^+q$ or $e^+g\to e^+g$ (HERA) [12,13], $p\bar{p}\to t\bar{t}+X$ (Tevatron) [11], and $M_D\gtrsim 1$ TeV via processes such as $q\bar{q},gg\to l^+l^-$ (Tevatron) and $e^+e^-\to f\bar{f}$ (LEP2) [9,13]. Future colliders such as the NLC and the LHC will be able to push these limits to several TeV's through the study of these signals. Clearly other new physics can also give rise to similar signals, so while a search for such signals may be used to bound TeV scale gravitation theories, to clearly identify gravitation as the source generally requires more extensive analysis, such as the study of angular distributions of final state particles (e.g. [9]).

It should also be noted that the predictions in virtual graviton processes have some uncertainties since they depend on the sum over the Kaluza-Klein (KK) tower of the massive excitations which is not fully determined without knowing the full quantum gravity theory.

In this paper we investigate another possible direct signal of strongly coupled low energy gravity via the process $e^+e^-\to e^+e^-G$ (G=spin 2 graviton) which proceeds predominantly through the t-channel $\gamma\gamma$ (or ZZ) fusion subprocesses $\gamma\gamma(ZZ)\to G$, as well as the related process $e^-\gamma\to e^-G$. In the case of the two photon fusion, the photons are produced virtually and since these photons tend to be collinear, the process $e^+e^-\to e^+e^-G$ is significantly enhanced compared to s-channel processes. We find that the resulting signal is robust and useful for detecting or constraining some low energy gravity scenarios at the energy scales of a future NLC.

Using this method, a 1 TeV electron-positron collider with integrated luminosity of 200 fb is sensitive to a gravitational scale of 2.8 TeV for 2 extra dimensions and 1.5 TeV for 6 extra dimensions. The main factors limiting the sensitivity are:

(1) The standard model background $e^+e^-\to e^+e^-\nu_e\bar{\nu}_e$ which leads to a final state with the same experimental signature.

(2) The necessity to observe the two electrons with a significant P_T in order to infer the existence of a missing particle (i.e., the graviton).

The rate of graviton production would be greatly enhanced if, instead of colliding two virtual photons, one were to collide two real photons produced via backscattering from the electron beams [10]. Unfortunately, in this case the process would be $\gamma\gamma\to G$ which would have no signal in the detector. On the other hand, if a laser only backscatters from one of the electron beams, then the process is $e^-\gamma\to e^-G$ and would give a signal of a single electron with a large unbalanced transverse momentum.

In this case the main limiting factor is the standard model background primarily from $e^-\gamma\to e^-\nu_e\bar{\nu}_e$. An election-positron collider with center of mass energy of 1 TeV which is converted to an electron-photon collider will thus be sensitive to a new gravitational scale of 10.4 TeV in the case of 2 extra dimensions and 2.7 TeV in the case of 6 extra dimensions.

In Sec. II we discuss the case of graviton production through $\gamma\gamma$ fusion at electron-positron colliders. In Sec. III we consider the case of $e^-\gamma\to e^-+\text{graviton}$ at an electron-photon collider and in Sec. IV we give our concluding remarks.

II. GRAVITON PRODUCTION BY TWO PHOTON FUSION

Let us first consider the excitation of spin 2 graviton modes through photon-photon and ZZ fusion. Such a process could be probed at an e^+e^- collider where the effective photon luminosity is generated by collinear photon emission. The complete process is therefore $e^+e^-\to e^+e^-G$ through the diagram shown in Fig. 1. In principle other diagrams where the graviton is attached to the fermion lines or directly to the gauge-fermion vertex will also contribute, but the process in Fig. 1 should be dominant due to the enhancement of collinear gauge boson emission.

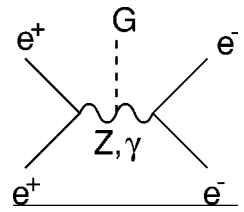

FIG. 1. The dominant Feynman diagram for $e^+e^-\to e^+e^-G$ through an effective photon or Z sub-process.

The cross section of the photon-photon fusion process may be estimated through the Weiszacker-Williams leading log approximation [17]. Thus if $\Sigma|\mathcal{M}(\hat{s})|^2$ is the matrix element for $\gamma\gamma\to G$, where G is a graviton of mass $m=\sqrt{\hat{s}}$, then in this approximation the total cross section for $e^+e^-\to e^+e^-G$ is given by

$$\sigma(e^+e^-\to e^+e^-G)=\frac{\pi\eta^2}{4s}\int_0^1\frac{f(\omega)}{\omega}D(\omega s)\sum|\mathcal{M}(\omega s)|^2d\omega \tag{3}$$

where s is the center of mass energy of the collision,

$$f(\omega)=[(2+\omega)^2\log(1/\omega)-2(1-\omega)(3+\omega)]/\omega$$

and $\eta=\alpha\log[s/(4m_e^2)]/(2\pi)$.

Using the effective Lagrangian for the $G\gamma\gamma$ coupling derived in [6,7], we obtain

$$\sum|\mathcal{M}(\hat{s})|^2=2\frac{\hat{s}^2}{M_D^2}. \tag{4}$$

Note that the explicit dependence on $\bar{M}_P$ will cancel when multiplied by the density of graviton states. This is typical of reactions involving real graviton emission. We therefore obtain the total cross section in this approximation:

$$\sigma_{\gamma\gamma}(e^+e^-\to e^+e^-G)=\frac{\alpha^2}{16\pi s}S_{\delta-1}\left[\sqrt{\frac{s}{M_D}}\right]^{\delta+2}F_{\delta/2}\log^2\left[\frac{s}{4m_e^2}\right] \tag{5}$$

where $F_k=\int_0^1 f(\omega)\omega^k d\omega$.

In Fig. 2, the solid curves give the total cross section as a function of s given $M_D=1$ TeV for $e^+e^-\to e^+e^-G$ in the cases where $\delta=2$ and 6 (corresponding to the upper and lower solid curves) while the thin dashed curve is the cross section for $\mu^+\mu^-\to\mu^+\mu^-G$ with $\delta=2$ which would be applicable to a muon collider. We see, for example, that if the gravitational interactions scale is 1 TeV, hundreds (thousands) of such e^+e^-G events will be produced already at LEP2 (at a 500 GeV NLC).

Experimental considerations suggest, however, that perhaps the full cross section which is given in the above is not observable. Gravitons couple very weakly to normal matter

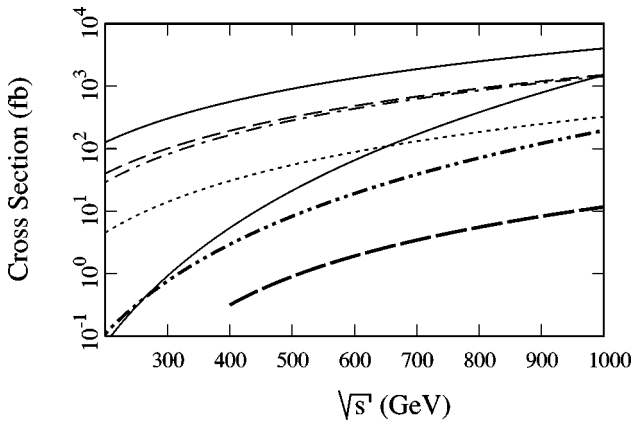

FIG. 2. The cross sections for $l^+l^-\to l^+l^-G$ for various values of δ are shown as a function of $\sqrt{s}$. The solid lines are the total cross sections for $e^+e^-\to e^+e^-G$ for $\delta=2$ (upper curve) and $\delta=6$ (lower curve). The dotted line is for the case that both the outgoing electrons are subject to the cut $P_{Tmin}=10$ GeV and for $\delta=2$. The dot-dash line is obtained again with $\delta=2$ but now only one of the outgoing electrons is subject to the cut $P_{Tmin}=20$ GeV. The thick dot-dot-dash line is for $\delta=4$ where both of the outgoing electrons are subject to the cut $P_{Tmin}=10$ GeV. The thick dashed line shows the total cross section for $\delta=2$ via the ZZ process. The dashed line gives the cross section for $\mu^+\mu^-\to\mu^+\mu^-G$ for $\delta=2$ via the $\gamma\gamma$ process. In all cases we take $M_D=1$ TeV.

and thus a radiated graviton will not be detected in the detector. Therefore, the signature for the reaction would be

$$e^+e^-\to e^+e^-+\text{missing mass}.$$

Since this cross section is dominated by emission of photons at a small angle, the outgoing electrons will therefore also be deflected by a small angle. Although one can expect that the electrons will suffer an energy loss, a significant portion of the electrons will not be deflected out of the area of the beam pipe and so may not be directly detected. To obtain a more realistic estimate one must therefore select events where the electron is deflected enough to be detected. Moreover, there is a standard model (SM) background to this signal from the processes $e^+e^-\to e^+e^-\nu_l\bar{\nu}_l$, $l=e,\ \mu,\ \tau$. We performed the exact tree-level calculation of this background by means of the COMPHEP package [18]. This background is found to be dominated by the $e^+e^-\nu_e\bar{\nu}_e$ final state; it is $\sim$420 fb for $\sqrt{s}=500$ GeV and $\sim$360 fb at $\sqrt{s}=1$ TeV (out of which $\sim$90% is from $e^+e^-\nu_e\bar{\nu}_e$), including all neutrino flavors and when no cuts are imposed.[2] Note that this background includes subprocesses where there are intermediate states of

[2]There is, in principle, additional reducible background, e.g., two photon production when one is lost down the beam pipe. Such a background is tied to the detailed specifications of the detector. We therefore consider it beyond the scope of this paper, however, it should be noted that it is expected to be much smaller than the SM irreducible background.

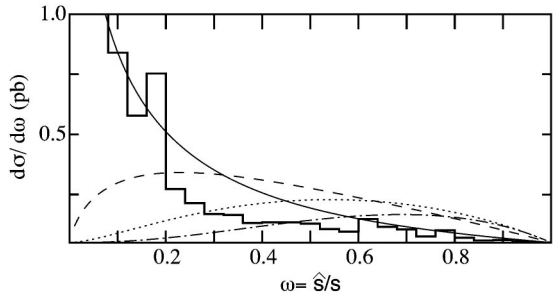

FIG. 3. The differential cross section as a function of the missing invariant mass squared ($\omega=\hat{s}/s$) for $\delta=2$ (solid line), $\delta=4$ (dashed line), $\delta=6$ (dotted line), $\delta=8$ (dot-dash line); for $M_D=1$ TeV, $P_{Tmin}=10$ GeV and $\sqrt{s}=1$ TeV. The standard model background from $e^+e^-\to e^+e^-\nu\overline{\nu}$ calculated by COMPHEP [18] is shown with the solid histogram.

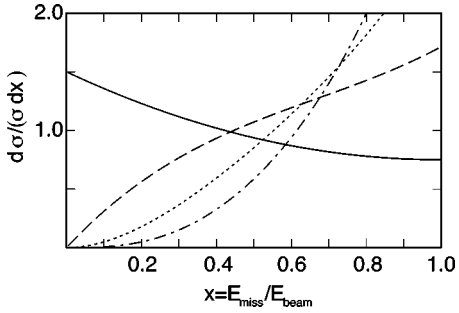

FIG. 4. The normalized differential cross section as a function of the missing energy of the single detected electron. See also caption to Fig. 3.

two gauge bosons such as $e^+e^-\to W^+W^-\to e^+\nu_e e^-\overline{\nu_e}$ and $e^+e^-\to Z\gamma\to\nu\overline{\nu}e^+e^-$. Tau-lepton pair production can also lead to a background with four neutrinos in the final state, specifically, $e^+e^-\to\tau^+\tau^-$ where each of the τ-leptons decays leptonically to $e\nu\overline{\nu}$. We find, however, that this gives a contribution which is about two orders of magnitude smaller than $ee\nu\nu$.

Let us now consider three possible methods for detection of this signal. First, one could take advantage of the fact that a significant amount of energy present in the initial collision is lost to the unobservable graviton. In Fig. 3, the missing mass distribution is shown as a function of $\omega=\hat{s}/s$ where $\hat{s}$ is the missing mass squared of the graviton. The results here are for the cut $P_T>10$ GeV with $\sqrt{s}=1$ TeV and $M_D=1$ TeV but, in this approximation, the shapes of the curves are not changed by the value of $\sqrt{s}$, M_D or any systematic cut imposed on the transverse momentum P_T of the outgoing electrons. The distribution is shown for $\delta=2$ (solid), $\delta=4$ (dashed), $\delta=6$ (dotted) and $\delta=8$ (dot-dash), where it is evident that, for the cases $\delta=4$, 6 and 8, the missing mass carried by the graviton is predominantly concentrated at high ω values. In contrast, the missing mass spectrum for the background discussed above (in particular, for the dominating background process $e^+e^-\to e^+e^-\nu_e\overline{\nu_e}$), which is also shown in Fig. 3, is somewhat peaked at low $\hat{s}$. Therefore, to obtain a bound on M_D it may also be useful to consider a cut on ω for the cases $\delta>2$. For example, for $\sqrt{s}=1$ TeV, the cut $\omega<0.16$ reduces the background by a factor of ~ 0.38, while the signal is reduced by a factor of 0.42 in the case of $\delta=2$, 0.82 in the case of $\delta=4$, 0.96 in the case of $\delta=6$ and 0.99 in the case of $\delta=8$. We will not consider further such a cut on ω.

It can be seen from Fig. 3 that the shape of the signal depends to a large extent on the number of extra dimensions present. The reason for this is apparent from Eq. (2) where the density of states is proportional to $\omega^{\delta/2-1}d\omega$ therefore the larger the value of δ, the higher the density at large ω and so the peak of the plot will tend to move to larger values of ω as δ is increased. If a signal is seen, therefore, the missing mass distributions in Fig. 3 will be helpful in determining the number of extra dimensions present. In addition, these distributions are relatively hard and will help distinguish this gravitational mechanism from other new physics candidates.

In principle it might be possible to separate the reduced energy electrons from the outgoing electrons of the collision at a e^+e^- collider through downstream dipole magnets but the large bremsstrahlung radiation generated by the disruption of the collision probably makes such an electron difficult or impossible to detect. At a muon collider, perhaps a Roman Pot could find reduced energy muons which were deflected from the main beam, however the decay electrons in the muon collider environment may make this difficult also. Clearly experimental innovations are required to detect the full cross section and we will not consider this further.

Secondly, if both of the electrons are given enough of a transverse momentum that they may be detected in the detector or the end-caps, events of the desired type may be identified. Using the leading log approximation, one can use Eq. (3) with η replaced by $\hat{\eta}(P_{Tmin})=\alpha\log[s/(4P_{Tmin}^2)]/(2\pi)$ where P_{Tmin} is the minimum transverse momentum of the outgoing electron which is accepted. If one imposes this cut on the two outgoing electrons one obtains the cross section as a function of $\sqrt{s}$ shown in Fig. 2 with the dotted curve for the case of $P_{Tmin}=10$ GeV with $M_D=1$ TeV and $\delta=2$, while the heavy dot-dot-dash curve is for $\delta=4$. These curves would be the same at both electron and muon colliders since the transverse momentum cut is well above the lepton mass. The missing mass spectra under this cut should also correspond to the curves shown in Fig. 3.

Thirdly, one could identify events where only one of the electrons has a transverse momentum greater than P_{Tmin}. This would in effect be replacing η^2 in Eq. (3) with $\eta_{eff}^2=\eta(P_{Tmin})(2\eta-\eta(P_{Tmin}))$. The resultant cross sections are shown in Fig. 2 with the dot-dash curve for $P_{Tmin}=20$ GeV. In this case, the energy of the detected electron will be markedly reduced from the beam energy since the graviton mass distribution increases at high masses. In Fig. 4 we show the normalized missing energy (E_{miss}) spectrum as a function of $x=2E_{miss}/\sqrt{s}=E_{miss}/E_{beam}$ for the detected electron where $\delta=2$ (solid), $\delta=4$ (dashed), $\delta=6$ (dotted) and $\delta=8$ (dot-dash). In this leading log approximation, the curves of Fig. 4 are largely independent of P_{Tmin}. For instance, if we impose the cut $x>0.2$, the signal is reduced by

TABLE I. The 3σ limits on the parameter M_D, as defined in Eq. (8), are given for $\delta=2$, 4 and 6. In each case three accelerator scenarios are considered: $\sqrt{s}=200$ GeV, 500 GeV and 1000 GeV with luminosities 2.5 fb^{-1}, 50 fb^{-1} and 200 fb^{-1}, respectively. The signals considered are based on the total cross section, the cross section with one electron passing the $P_{Tmin}=10$ GeV cut and the cross section with both electrons passing the $P_{Tmin}=10$ GeV cut.

		$\delta=2$		
$\sqrt{s}$	$\int \mathcal{L}dt$	No cut	$P_{Tmin}=10$ GeV (one electron)	$P_{Tmin}=10$ GeV (two electrons)
200 GeV	2.5 fb^{-1}	1.3 TeV	1.0 TeV	0.6 TeV
500 GeV	50 fb^{-1}	2.8 TeV	2.4 TeV	1.7 TeV
1000 GeV	200 fb^{-1}	4.1 TeV	3.6 TeV	2.8 TeV
		$\delta=4$		
$\sqrt{s}$	$\int \mathcal{L}dt$	No cut	$P_{Tmin}=10$ GeV (one electron)	$P_{Tmin}=10$ GeV (two electrons)
200 GeV	2.5 fb^{-1}	0.7 TeV	0.5 TeV	0.4 TeV
500 GeV	50 fb^{-1}	1.6 TeV	1.4 TeV	1.0 TeV
1000 GeV	200 fb^{-1}	2.5 TeV	2.3 TeV	1.9 TeV
		$\delta=6$		
$\sqrt{s}$	$\int \mathcal{L}dt$	No cut	$P_{Tmin}=10$ GeV (one electron)	$P_{Tmin}=10$ GeV (two electrons)
200 GeV	2.5 fb^{-1}	0.5 TeV	0.4 TeV	0.3 TeV
500 GeV	50 fb^{-1}	1.1 TeV	1.0 TeV	0.8 TeV
1000 GeV	200 fb^{-1}	1.9 TeV	1.8 TeV	1.5 TeV

a factor of 0.72 in the case of $\delta=2$, 0.93 in the case of $\delta=4$, 0.99 in the case of $\delta=6$ and 0.997 in the case of $\delta=8$. We will not use this cut in our numerical results below, however, again, if a signal is seen, the missing energy distributions in Fig. 4 may provide an extra handle in resolving the origin of such a signal.

Let us now consider the related process $e^+e^- \to ZZe^+e^- \to e^+e^-G$ which can likewise be estimated by the effective vector boson leading log approximation. In general the cross section is given by a sum over cross sections for $ZZ \to G$ in various helicity combinations together with the helicity dependent structure functions given in [19,20] (in particular we use the formulation of [20]). Here there is considerable simplification since in this approximation where the boson momenta are taken collinear with their parent leptons, the only amplitude which contributes are the cases where the bosons are transverse and of opposite helicities. As with the photon case, we use the effective Lagrangian from [6] and obtain the cross section in this approximation:

$$\sigma_{ZZ}(e^+e^- \to e^+e^-G) = \frac{y^2\alpha^2}{16\pi s} S_{\delta-1}\left(\frac{\sqrt{s}}{M_D}\right)^{\delta+2} [F^Z_{\delta/2}(s) + z^2 H^Z_{\delta/2}(s)] \log^2\left(\frac{s}{M_Z^2}\right) \quad (6)$$

where

$$x_w = \sin^2\theta_w, \quad y = \frac{1-4x_w+8x_w^2}{8x_w(1-x_w)}, \quad z = \frac{1-4x_w}{2(1-4x_w+8x_w^2)},$$

$$F^Z_k(s) = \int_{4m_Z^2/s}^1 \omega^k f(\omega) d\omega$$

$$H^Z_k(s) = -\int_{4m_Z^2/s}^1 4\omega^k \left[(4+\omega)\log\left(\frac{1}{\omega}\right) - 4(1-\omega)\right] \quad (7)$$

and $f(\omega)$ is defined as for the case of photons.

In Fig. 2 the thick dashed curve shows the total cross section for this process given $M_D=1$ TeV and $\delta=2$. Clearly, the ZZ-fusion cross section is much smaller than the two photon process.[3] Moreover, this cross section is flat in P_T for $P_T < O(m_Z)$ and therefore $O(10$ GeV) cuts in P_T of the outgoing leptons will not reduce this greatly. For similar reasons the cross section at a $\mu\mu$ collider will be the same.

[3]We note that, for massive vector bosons, the effective vector boson approximation in leading log tends to overestimate the cross section, in particular, the cross section coming from fusion of transversely polarized gauge bosons, see e.g., Johnson *et al.* in [21]. However, since the photon-photon process is much larger than the ZZ even when the latter is calculated in the leading log approximation, this effect is negligible for our numerical results.

In Table I we consider the limits that may be placed on theories with extra dimensions using these $e^+e^-\to e^+e^-G$ processes in case no such signal is detected. We consider three possible accelerator scenarios: $\sqrt{s}=200$ GeV and a total integrated luminosity of 2.5 fb^{-1} (for LEP-200); $\sqrt{s}=500$ GeV and a total integrated luminosity of 50 fb^{-1}; $\sqrt{s}=1$ TeV and a total integrated luminosity of 200 fb^{-1}. These last two cases correspond to a future NLC. For $\delta=2$, 4 and 6 we consider detection either via the full cross section (if that were somehow observable) or via the signal with the cut $P_{Tmin}=10$ GeV on just one outgoing electron or both outgoing electrons.

We define the lower limit on M_D in each case to be the value which will yield a signal with a statistical significance of 3σ above the background by requiring

$$\frac{\sigma^T-\sigma^{SM}}{\sqrt{\sigma^T}}\times\sqrt{L}>3, \tag{8}$$

where σ^T is the total cross section for e^+e^- + missing energy production and σ^{SM} is the SM contribution to this signal. L is the luminosity of the collider and we also require (for the given L) at least 10 such e^+e^-G events above the SM background for the given lower bound on M_D.[4] The limits given by Eq. (8) include only the effects of statistical error. In general there will also be some accelerator and detector dependent systematic errors which will tend to reduce these bounds; these we have not included throughout this paper.

As can be seen, in the case of two extra dimensions and using the signal with the two electron P_{Tmin} cuts, a limit of about 600 GeV may be placed on M_D at the 200 GeV collider; using the 500 GeV collider a limit of about 1.7 TeV may be obtained and with a 1 TeV collider a limit of about 2.8 may result. Thus, in general, a given collider (out of the three scenarios above) can place a 3σ bound on M_D of about three times its c.m. energy. Obviously, with less stringent cuts and/or using a single high P_T lepton tag, the lower limit on M_D may be increased. Also, we note that, as expected, the limit on M_D decreases somewhat as δ increases and that, as mentioned before, a lower cut on the missing mass may be of some advantage if $\delta>2$.

The background may be reduced by considering right polarized electron beams (with left polarized positron beams) which has the effect of eliminating the diagram with a WW fusion topology [24]. For instance, if a right polarization of 90% is considered, the given bounds on M_D for $\delta=2$ are improved by about 30%, for $\delta=4$ they are improved by about 20% and for $\delta=6$, by about 15%.

[4]In fact, we find that, using the 3σ lower bounds on M_D as given in Table I and the given colliders luminosities, about 50–100 e^+e^-G events will be produced at LEP2 energies, while hundreds –thousands such events will emerge at 500 and 1000 GeV NLC, for all three values of δ considered in Table I.

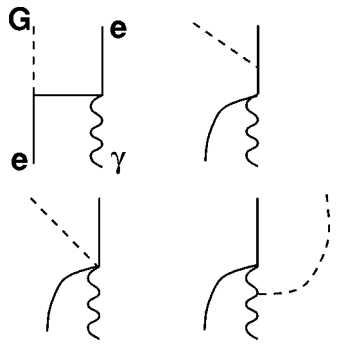

FIG. 5. The dominant Feynman diagrams for $e^-\gamma\to e^-G$.

III. GRAVITON PRODUCTION BY ELECTRON-PHOTON COLLISIONS

It has been suggested [10] that an electron-positron collider might be converted to an electron-photon or photon-photon collider by scattering a laser beam from one or both of the electron beams. This would produce a great enhancement over the virtual photon luminosities considered above. If a photon-photon collider were used, however, the production of gravitons could not be considered as above since the method requires observation of outgoing electrons to infer that a graviton was produced. On the other hand, at an electron-photon collider, the process $e^-\gamma\to e^-G$ would lead to a high transverse momentum electron in the final state which could be detected. The signature for such an event would therefore be $e^-\gamma\to e^-+P_T^{miss}$ where the missing transverse momentum is the same in the lab and in the $e\gamma$ rest frame.

As shown in Fig. 5, this process could proceed through several diagrams in addition to the one analogous to the fusion process considered above. This leads to the differential hard cross section in the $e^-\gamma$ center of mass frame for producing a graviton of mass m:

$$\frac{d\sigma(m)}{dz}=\frac{\pi\alpha G_N}{4(1-z^2)}(4(1+z)+x(1-z))\times(5-6x+5x^2+2z(1-x^2)+z^2(1-x)^2) \tag{9}$$

where $z=\cos\theta_{ee}$, θ_{ee} being the angle between the initial and final electron momenta in the center of mass frame and $x=m^2/s$ where s is the center of mass energy of the collision and G_N is the Newtonian gravitational constant. This formula is related by crossing symmetry to that derived in [4] for $e^+e^-\to\gamma G$. This distribution must be convoluted with the density of states in Eq. (2).

In the experimental setting where the photon beam is produced by laser backscatter, the energy of the photon in a specific event is not known. Since the missing mass is also

unknown, the event cannot be fully reconstructed and the distribution in z cannot be directly observed. It is more useful therefore to consider the distribution in the transverse momentum of the electron, P_T, or equivalently the missing transverse momentum P_T^{miss} which is given by $P_T = (\sqrt{s}/2)(1-x)\sqrt{1-z^2}$.

Convoluting the differential cross section in Eq. (9) with the density of states, we obtain the following differential cross section summed over graviton states:

$$\frac{d\sigma}{dz} = \frac{\alpha S_{\delta-1}}{64s}\left(\sqrt{\frac{s}{M_D}}\right)^{\delta+2} \frac{A_\delta + B_\delta z + C_\delta z^2 + D_\delta z^3}{1-z^2} \quad (10)$$

where A_δ, B_δ, C_δ and D_δ are given by

$$A_\delta = \int_0^1 (x+4)(5-6x+5x^2)x^{\delta/2-1}dx$$

$$B_\delta = \int_0^1 (28-27x+18x^2-7x^3)x^{\delta/2-1}dx$$

$$C_\delta = \int_0^1 3(1-x)(4+x-x^2)x^{\delta/2-1}dx$$

$$D_\delta = \int_0^1 (4-x)(1-x)^2 x^{\delta/2-1}dx. \quad (11)$$

We must now convolute this distribution with the energy spectrum of the photons in the collider to obtain the cross section relative to the e^+e^- luminosity. The distribution in terms of the energy fraction $u = E_\gamma/E_e$ given in [10] for laser photons scattered from an unpolarized electron beam is

$$f(u) = \frac{1/(1-u) + (1-u) - 4r(1-r)}{(1-4/X-8/X^2)\log(1+X) + 1/2 + 8/X - 1/(2(1+X)^2)} \quad (12)$$

where $u \leqslant u_{max} = X/(X+1)$, $r = u/(X(1-u))$ and $X = 4E_e\omega_0/m_e^2$, E_e being the energy of the scattering electron beam and ω_0 being the energy of the laser photons.

The total cross section with respect to the e^-e^+ luminosity is

$$\sigma_0 = \int_0^{u_{max}} \sigma_{e\gamma}(s_0 u) f(u) du \quad (13)$$

where s_0 is the center of mass energy that the e^+e^- system has without laser scattering.

The number of events is thus $N = \sigma_0 \mathcal{L}_{ee}$ where $\mathcal{L}_{ee}$ is the integrated luminosity for e^+e^- collisions if the scattering laser were absent.

The above result assumes that ω_0 is not so large as to cause e^+e^- pairs to be created in the scattering. This is equivalent to $X \leqslant 2(1+\sqrt{2})$. We therefore take $X = 2(1+\sqrt{2})$ which gives the hardest spectrum without pair generation. For instance, in the case where $\sqrt{s_0} = 1$ TeV, this value of X corresponds to $\omega_0 = 0.63$ eV.

In Fig. 6 we show $d\sigma_0/dP_T$ for a collider where $\sqrt{s_0} = 1$ TeV in the cases $\delta = 2$ (upper solid), 4 (dotted), 6 (dashed) and 8 (dot dashed) together with the SM background (lower solid) calculated with the COMPHEP package [18]. In this case the background comes from $e^-\gamma \to e^-\nu_l\bar{\nu}_l$ where $l = e$, μ and τ. As before, the dominant background is generated by $l = e$.

The background may also be suppressed by polarizing the electron beam with a right handed helicity [24]. This eliminates the contribution of graphs which have a virtual W exchange that provide the dominant component in the unpolarized case. In Fig. 6, the lower two background curves are the P_T distributions with 90% and 100% right polarizations as indicated.

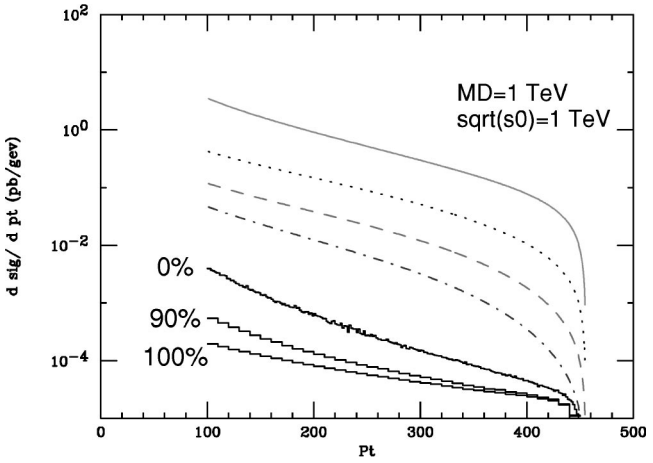

FIG. 6. The distribution $d\sigma_0/dP_T$ for the signal and SM background when $\sqrt{s_0} = 1$ TeV and $M_D = 1$ TeV. The photons are produced by the backscatter of a laser where $X = 2(1+\sqrt{2})$ and the electron beams are taken to be unpolarized. The signal is shown for $\delta = 2$ (upper solid curve); $\delta = 4$ (dotted curve); $\delta = 6$ (dashed curve) and $\delta = 8$ (dash dot curve). The SM background from $e^-\gamma \to e^-\nu_l\bar{\nu}_l$ is shown with the lower three solid curves. The largest background curve is for the case of an unpolarized electron beam. The two below are for 90% and 100% right polarized electron beams respectively.

TABLE II. The 3σ limits on the parameter M_D, as defined in Eq. (8), are given for $\delta=2$, 4 and 6 using the process $e^-\gamma\to e^-G$ where the electron beams are assumed to be unpolarized. In each case three accelerator scenarios are considered: $\sqrt{s_0}=500$ GeV, 1000 GeV and 1500 GeV with e^+e^- luminosities 50 fb^{-1}, 200 fb^{-1} and 200 fb^{-1}, respectively. In all cases we apply the cut $P_{Tmin}=\sqrt{s_0}/10$. The numbers in brackets indicate the results which could be obtained if the electron beam was right polarized 90%.

$\sqrt{s_0}$	$\int\mathcal{L}_{ee}dt$	$\delta=2$	$\delta=4$	$\delta=6$
500 GeV	50 fb^{-1}	5.5 (7.2) TeV	2.2 (2.6) TeV	1.3 (1.5) TeV
1000 GeV	200 fb^{-1}	10.4 (13.8) TeV	4.2 (5.1) TeV	2.7 (3.1) TeV
1500 GeV	200 fb^{-1}	14.0 (18.5) TeV	5.8 (7.0) TeV	3.8 (4.4) TeV

In Table II we give the 3-σ limit that may be obtained on M_D for $\delta=2$, 4 and 6 for collider scenarios with $\sqrt{s_0}=500$ GeV and $\mathcal{L}=50$ fb^{-1}; $\sqrt{s_0}=1000$ GeV and $\mathcal{L}=200$ fb^{-1} and $\sqrt{s_0}=1500$ GeV and $\mathcal{L}=200$ fb^{-1}. We also impose an acceptance cut of $P_T>\sqrt{s_0}/10$. The numbers in brackets are those which may be obtained under the same assumptions with a 90% right polarized electron beam.

In the case of $\delta=2$ fairly stringent bounds of 5.5(7.2) TeV, 10.4(13.8) TeV and 14.0(18.5) TeV can be placed on the scale of gravitational interactions for $\sqrt{s_0}=500$ GeV, 1000 GeV and 1500 GeV, respectively using unpolarized (90% right polarized) beams. This, is comparable, particularly in the polarized case, with the bounds for $\delta=2$ that have been obtained from supernova cooling [22] ($\sim$13 TeV), but much less than the bounds that may follow from the absence of diffuse cosmic gamma ray backgrounds [23] ($\sim$100 TeV). For larger δ where the astrophysical results do not apply, fairly stringent bounds may be placed on M_D. For instance, in the case of $\delta=4$ we obtain the bound of 2.2(2.6) TeV, 4.2(5.1) TeV, 5.8(7.0) TeV for $\sqrt{s_0}=500$ GeV, 1000 GeV and 1500 GeV, respectively for unpolarized (90% right polarized) electron beams.

IV. CONCLUSION

In conclusion, we have shown that effective photon-photon and real photon-electron collisions can produce massive gravitons at appreciable rates in theories with large extra dimensions where the gravitation scale is $1-10$ TeV. In the case of two photon fusion, the standard model background from $e^+e^-\to e^+e^-\nu_e\bar{\nu}_e$ limits the effectiveness somewhat but, for instance at a 1 TeV collider with integrated luminosity 200 fb^{-1} we are sensitive to a gravitation scale of $M_D=2.8$ TeV in the case where $\delta=2$ and 1.5 TeV in the case where $\delta=6$ taking a cut of $P_{Tmin}=10$ GeV on both the outgoing electrons.

The case of electron-photon fusion at an electron-photon collider is limited to a lesser extent by the standard model background $e^-\gamma\to e^-\nu_e\bar{\nu}_e$. Using this case at an electron-photon collider based on an electron-positron collider with center of mass energy of 1 TeV, a gravitation scale up to 10.4 TeV may be probed in the case of $\delta=2$ and 2.7 TeV in the case of $\delta=6$. These results may be somewhat improved through the use of polarized electron beams.

Note added in proof. After submission of this paper we came across some related recent works [25].

ACKNOWLEDGMENTS

We are grateful to Jose Wudka for discussions. One of us (D.A.) thanks the UCR Theory Group and the Fermilab Theory Group for hospitality. This research was supported in part by US DOE Contract Nos. DE-FG02-94ER40817 (ISU), DE-FG03-94ER40837 (UCR) and DE-AC02-98CH10886 (BNL).

[1] P. Horava and E. Witten, Nucl. Phys. **B460**, 506 (1996); **B475**, 94 (1996); E. Witten, *ibid.* **B471**, 135 (1996); I. Antoniadis, Phys. Lett. B **246**, 377 (1990); P. Ginsparg, *ibid.* **197**, 139 (1987).

[2] N. Arkani-Hamed, S. Dimopoulos, and G. Dvali, Phys. Lett. B **429**, 263 (1998); I. Antoniadis, N. Arkani-Hamed, S. Dimopoulos, and G. Dvali, *ibid.* **436**, 257 (1998).

[3] J. Lykken, Phys. Rev. D **54**, 3693 (1996); J. Dienes, E. Dudas, and T. Ghergetta, Phys. Lett. B **436**, 55 (1998); G. Shiu and S. H. Tye, Phys. Rev. D **58**, 106007 (1998); N. Arkani-Hamed, S. Dimopoulos, and J. March-Russell, Phys. Rev. D (to be published), hep-th/9908146; hep-th/9809124.

[4] E. A. Mirabelli, M. Perelstein, and M. E. Peskin, Phys. Rev. Lett. **82**, 2236 (1999).

[5] V. P. Mitrofanov and O. I. Ponomareva, Zh. Éksp. Teor. Fiz. **94**, 16 (1988) [Sov. Phys. JETP **67**, 1963 (1988)]; J. C. Long, H. W. Chan, and J. C. Price, Nucl. Phys. **B539**, 23 (1999), and references therein.

[6] G. F. Giudice, R. Rattazzi, and J. D. Wells, Nucl. Phys. **B544**, 3 (1999).

[7] T. Han, J. D. Lykken, and R. Zhang, Phys. Rev. D **59**, 105006 (1999).

[8] S. Nussinov and R. Shrock, Phys. Rev. D **59**, 105002 (1999).

[9] J. L. Hewett, Phys. Rev. Lett. **82**, 4765 (1999).

[10] I. F. Ginzburg, G. L. Kotkin, V. G. Serbo, and V. I. Telnov, Nucl. Instrum. Methods Phys. Res. **205**, 47 (1983); I. F. Ginzburg, G. L. Kotkin, S. L. Panfil, V. G. Serbo, and V. I. Telnov, Nucl. Instrum. Methods Phys. Res. A **219**, 5 (1984).

[11] P. Mathews, S. Raychaudhuri, and K. Sridhar, Phys. Lett. B **450**, 343 (1999).

[12] P. Mathews, S. Raychaudhuri, and K. Sridhar, Phys. Lett. B **455**, 115 (1999).

[13] T. G. Rizzo, Phys. Rev. D **59**, 115010 (1999).
[14] K. Agashe and N. G. Deshpande, Phys. Lett. B **456**, 60 (1999).
[15] K. Cheung and W. Keung, Phys. Rev. D **60**, 112003 (1999).
[16] T. G. Rizzo, Phys. Rev. D **60**, 075001 (1999).
[17] See, e.g., M. Peskin and D. Schroeder, *An Introduction to Quantum Field Theory* (Addison-Wesley, Reading, MA, 1995), p. 578.
[18] P. A. Baikov *et al.*, Physical Results by means of CompHEP, in Proceedings of the 10th Workshop on High Energy Physics and Quantum Field Theory (QFTHEP-95), edited by B. Levtchenko and V. Savrin, Moscow, 1996, p. 101, hep-ph/9701412; E. E. Boos *et al.*, hep-ph/9503280. The CompHEP package Version 33 was downlowded from the Web page: http://theory.npi.msu.su/comphep.html.
[19] See, e.g., S. Dawson, Nucl. Phys. **B249**, 42 (1985); R. P. Kauffman, Phys. Rev. D **41**, 3343 (1990); M. S. Chanowitz and M. K. Gailard, Phys. Lett. **142B**, 85 (1984); G. L. Kane, W. W. Repko, and W. R. Rolnick, *ibid.* **148B**, 367 (1984).
[20] V. D. Barger and R. J. N. Phillips, *Collider Physics* (Addison-Wesley, Reading, MA, 1987).
[21] P. W. Johnson, F. I. Olness, and W. K. Tung, Phys. Rev. D **36**, 291 (1987).
[22] S. Cullen and M. Perelstein, Phys. Rev. Lett. **83**, 268 (1999); V. Barger, T. Han, C. Kao, and R. J. Zhang, Phys. Lett. B **461**, 34 (1999).
[23] L. J. Hall and D. Smith, Phys. Rev. D **60**, 085008 (1999).
[24] Hong-Jian He (private communication).
[25] D. Ghosh *et al.*, hep-ph/9909377; hep-ph/9909567.